Central European Journal of Energetic Materials, **2015**, *12*(3), 487-495
ISSN 1733-7178
e-ISSN 2353-1843

Process Optimization and Characterization of an HMX/Viton Nanocomposite

Xiaofeng SHI [1,*], Cailing WANG [2], Jingyu WANG [3], Xiaodong LI [3], Chongwei AN [3], Jiang WANG [3], Wei JI [3]

[1] Shuozhou, North University of China, Shuozhou Shanxi, 030051, P. R. China
[2] Xi'an Modern Chemistry Research Institute, Xi'an Shanxi, 710065, P. R.China
[3] Chemical Industry and Ecology Institute, North University of China, Taiyuan Shanxi, 030051, P. R. China
[*]E-mail: profound_000@163.com

Abstract: HMX/Viton A nanocomposites were prepared by a spray drying process using different processing parameters, which included the dry gas inlet temperature, the air flow rate, and the solution feed flow rate. Scanning electron microscopy (SEM) and X-ray diffraction (XRD) were used to characterize the nanocomposites. The effects of the processing parameters on the morphology of the samples were investigated and are discussed. The thermal decomposition behaviour and impact sensitivity of the raw HMX and HMX/Viton A nanocomposites were also measured and compared. Optimal morphology and dispersion of the coated samples was achieved when the dry gas inlet temperature and the air and solution feed flow rates were 55 °C, 660 L/h and 1.5 mL/min, respectively. Under these optimal processing conditions, the nanocomposites were spherical in shape, ranged from 0.2-2 μm in size, and were composed of many tiny particles of 50-100 nm in size. The crystal phase of the nanocomposites was the same as that of raw HMX. Compared with those of raw HMX, the melting point and impact sensitivity of the nanocomposites were lower and the thermal decomposition rate was slightly higher.

Keywords: HMX, spray drying, processing parameters, optimization, impact sensitivity, nanoparticles

1 Introduction

There has been strong recent interest in energetic nanocomposites because they have the advantages of both nano-sized energetic materials and additives. HMX (1,3,5,7-tetranitro-1,3,5,7-tetrazocane) based spherical nanocomposites using Viton A as a binder have many advantages. Firstly, nano-sized particles of explosives cannot only have reduced mechanical sensitivity [1-4], but also an enhanced burning rate compared with the bulk material [5, 6]. However, they have one disadvantage – a reduced shelf life [7]. Energetic nanocomposites can overcome this problem to some extent. Secondly, Viton A is a type of high molecular weight polymer which provides sufficient strength, superior mechanical performance, and improves the ageing, heat-resistance, and corrosion resistance of materials when used as a binder [8], so the mechanical properties of HMX-based Viton A energetic nanocomposites are excellent [9]. Thirdly, spherical particles of explosives can also have reduced mechanical sensitivity [10, 11].

Energetic spherical nanocomposites can be prepared using spray drying methods [12-16]. However, there are great differences in the morphology of the particles produced under different processing parameters. In particular, particles may suffer from obvious holes and cracks under some conditions. These defects easily form "hot spots", which increase the mechanical sensitivity of the energetic material [17-19]. In the present work, we prepared HMX/Viton A energetic spherical nanocomposites by spray drying and optimized the processing parameters to decrease the number of defects in the samples. The influence of the spray drying conditions on the properties of the HMX/Viton A energetic spherical nanocomposites was studied in detail.

2 Experimental

2.1 Materials

β-HMX was provided by the Modern Chemistry Research Institute of China, acetone was purchased from Shanghai Chemical Ltd., China, and Viton A was received from Huizhou HaoYuan Plastic Raw Material Co., Ltd., China.

2.2 Preparation of HMX based composite energetic microspheres

Initially, appropriate amounts of HMX and Viton A were dissolved in acetone under ultrasonication to form the spray drying precursor solution. The mass ratio of HMX to Viton A was 98:2 and the solution mass concentration was 2%. The processing parameters of a mini Buchi 290 spray dryer (BUCHI

Labortechnik AG; nozzle dimension: 0.7 mm; three variables, dry gas inlet temperature, air flow rate, and feed solution flow rate) were then set at the desired values. The solution was sprayed and dried in an electrically-grounded glass collection vessel to obtain the nanocomposites.

2.3 Instruments and apparatus

A DX-2700 diffractometer (Dandong Haoyuan Instrument Co., Ltd., China) was used to investigate the crystal phases of the raw HMX and the HMX/Viton A nanocomposites by X-ray diffractometry (XRD). The morphology and size of the HMX-based nanocomposites were studied using a Hitachi S-4800 scanning electron microscope (SEM; Hitachi Ltd., Japan). Differential scanning calorimetry (DSC) experiments were conducted under a N_2 atmosphere using a Setaram DSC131 instrument (Setaram instrumentation Co., France). The test conditions were: sample mass, 0.7 mg; N_2 flow rate, 15 mL/min and sample heating rate, 20 K/min. The impact sensitivity of the HMX/Viton A nanocomposites was tested at room temperature using an ERL type 12 drop hammer apparatus with a sample mass of 35 ± 1 mg and a drop weight of 5 ± 0.002 kg. Four groups of each sample and 25 identical specimens from each group were tested. The results are described in terms of the critical drop-height of 50% explosion probability (H_{50}) and the standard deviation (S).

3 Results and Discussion

3.1 Influence of processing parameters on sample morphology

The processing parameters (dry gas inlet temperature, air flow rate, feed solution flow rate) had significant effects on the morphology and distribution of the products obtained. The experimental scheme is listed below (Table 1). The morphology of the particles prepared under different process parameters were compared.

Table 1. Process parameters used in each experiment

PP [a]	E1 [e]	E2 [e]	E3 [e]	E4 [e]	E5 [e]	E6 [e]	E7 [e]
Temp [b], [°C]	55	75	85	55	55	55	55
FA [c], [L/h]	430	660	660	280	660	660	660
FF [d], [mL/min]	1.5	1.5	1.5	1.5	1.5	4.5	7.5

[a] PP: processing parameter; [b] Temp: temperature of dry gas inlet; [c] FA: air flow rate; [d] FF: flow rate of feed solution; [e] E1-E7: experiments 1-7.

3.1.1 Temperature of dry gas inlet

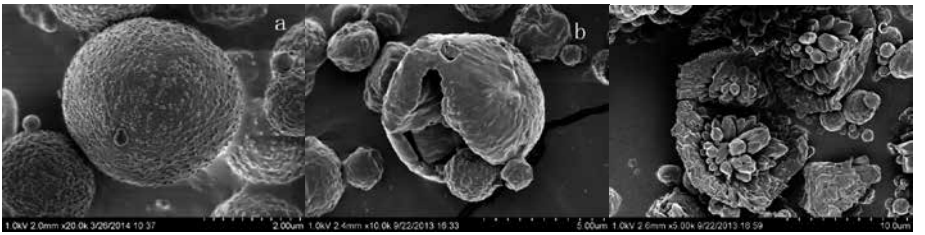

Figure 1. SEM images of coated HMX samples produced at different temperatures of the dry gas inlet: a) 55 °C; b) 75 °C; c) 85 °C.

As is shown in Figure 1, three samples were prepared by spray drying at different dry gas inlet temperatures (E5, E2 and E3). The particles produced at a dry gas inlet temperature of 55 °C were spherical and without cracks (Figure 1a). The microspheres were composed of many tiny particles, most of which were 50-100 nm in size. The particles obtained at 75 °C were also spherical but exhibited large surface cracks (Figure 1b). As shown in Figure 1c, the particles obtained at 85 °C were ruptured and flower-like in shape. These results were caused by the acceleration in the speed of evaporation with the increase in the dry gas inlet temperature. When the evaporation rate is faster than the rate of solid spreading into the droplets, the droplets swell, break, or even split. This splitting generates dense solid fragments. However, if the dry gas inlet temperature is lower than 55 °C, the solvent (acetone) may not be evaporated completely. Hence, the particle shape of the sample obtained at 55 °C, shown in Figure 1a, was considered to be the optimum achievable.

3.1.2 Air flow rate

As shown in Figure 2, three samples were prepared by spray drying at different cyclone flow rates (E4, E1 and E5). Figures 2b and 2c show that the particles obtained at 430 and 660 L/h were spherical and did not have hollows on their surfaces. In Figure 2a however, many hollows are clearly visible on the surface of the particles produced at 280 L/h. The degree of droplet dispersion decreased with the speed of the air flow, resulting in larger droplets. When the vapour ressure inside the large droplets is greater than that outside the sphere, the wet bulb shell breaks. This caused the products to have irregular shapes. No further decrease in particle size was obvious when the air flow rate was greater than 660 L/h, so the optimum air flow rate was chosen as 660 L/h.

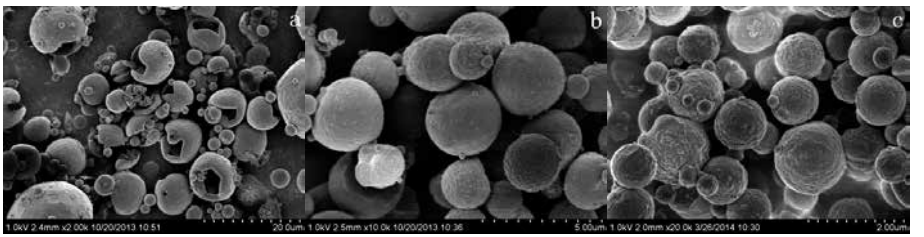

Figure 2. SEM images of coated HMX samples prepared at different cyclone flow rates: a) 280 L/h; b) 430 L/h; c) 660 L/h.

3.1.3 Flow rate of feed solution

Three samples were prepared by spray drying at different flow rates of the feed solution (E5, E6 and- E7). As is shown in Figure 3, the three samples were all spherical in shape, but had different particle sizes. The particle sizes of the samples ranged from 0.2-2 μm, 0.5-3.5 μm, and 1-4 μm for the samples prepared at flow rates of 1.5, 4.5, and 7.5 mL/min, respectively. Compared with the samples produced at feed solution flow rates of 4.5 and 7.5 mL/min (Figures 3b and 3c), the particles produced at 1.5 mL/min (Figure 3a) exhibited the most homogeneous size distribution. This can be explained as the dispersion of the droplets being ameliorated, tiny droplets being more likely to form at lower flow rates of the feed solution. The particle size of the samples did not obviously change if the flow rate of the feed solution was set lower than 1.5 mL/min. Thus, the optimum flow rate was chosen to be 1.5 mL/min.

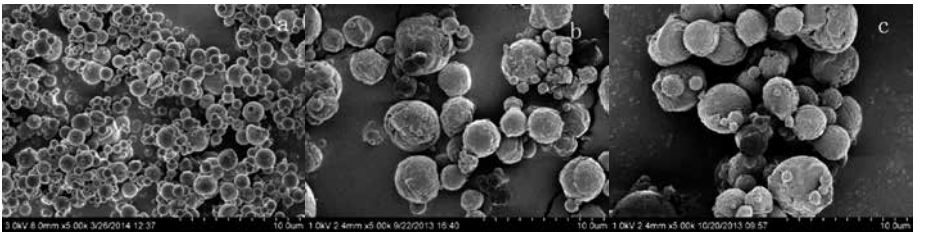

Figure 3. SEM images of coated HMX samples prepared at different flow rates of the feed solution: a) 1.5 mL/min; b) 4.5 mL/min; c) 7.5 mL/min.

3.2 XRD characterization

X-ray diffraction was used to study the crystal structure of the particles prepared using the E5 process parameters (marked as the optimized sample). Figure 4 indicates that this HMX-based nanocomposite displayed peaks at similar diffraction angles as those of the raw HMX, but additionally a number of unidentifiable diffraction peaks because of the addition of Viton A. Furthermore,

the peaks of the HMX/Viton A nanocomposite were much weaker and broader than those of the raw HMX, attributed to the decreased crystal size of the nanocomposite [20].

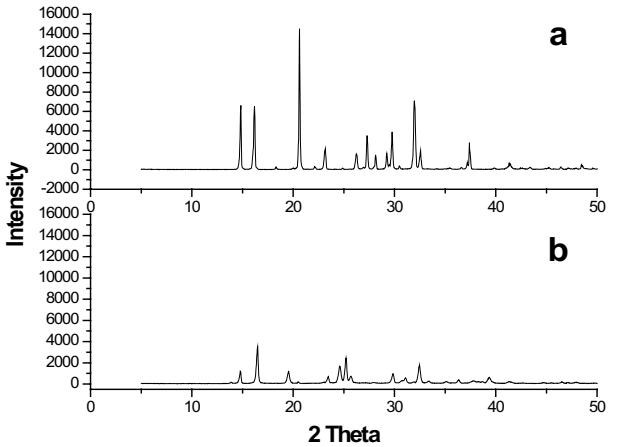

Figure 4. X-ray diffraction pattern of (a) raw HMX, and (b) HMX/Viton A nanocomposite.

3.3 Thermal Decomposition Characteristics

The raw HMX and the optimized nanocomposite sample were also studied by DSC. The DSC thermographs, obtained at a heating rate of 20 K/min, are shown in Figure 5.

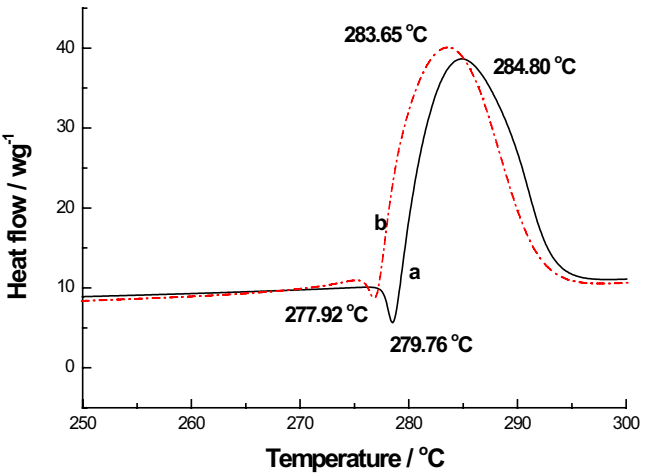

Figure 5. DSC curves of (a) raw HMX, and (b) HMX/Viton A nanocomposite at a heating rate of 20 K/min.

The DSC curves of raw HMX and HMX/Viton A exhibited an endothermic peak at 279.76 and 277.92 °C, respectively. This implies that the HMX began to melt at about 277-279 °C and that the melting point of the HMX/Viton A nanocomposite was lower than that of raw HMX. This is because reducing the particle size of a material to the nano-scale reduces its melting point. Meanwhile, the exothermic peak temperature of the HMX/Viton A nanocomposite was a little lower than that of raw HMX, indicating that the thermal decomposition rateof the HMX/Viton A nanocompositewas slightly faster than that of raw HMX, but not significantly so.

3.4 Impact Sensitivity

The mechanical sensitivity results of raw HMX and the optimized nanocomposite sample are listed in Table 2.

Table 2. Impact sensitivity of raw HMX and HMX/Viton A

Sample	Impact sensitivity [H_{50}]/cm				
	E1 [a] (S [b])	E2 [a] (S)	E3 [a] (S)	E4 [a] (S)	Average
Raw HMX	17.5 (0.09)	19.8 (0.06)	17.8 (0.05)	18.5 (0.06)	18.4
HMX/Viton A	56.2 (0.04)	53.6 (0.06)	55.7 (0.06)	58.4 (0.04)	56.0

[a] E1-E4: experimental group 1- 4; [b] S: standard deviation.

Table 2 shows that the drop height of HMX/Viton A is higher than raw HMX. This indicates that the impact sensitivity of HMX/Viton A is better than raw HMX, which is because Viton A can provide a shock absorber or diverter of mechanical stimuli. The tiny particle size and spherical shape of the sample can also decrease the mechanical sensitivity. The results show that HMX/Viton A possesses an outstandingly insensitive character.

4 Conclusions

Using 2% Viton A as a binder, HMX based nanocomposites were prepared by a spray drying method. The temperature of the dry gas inlet and the flow rates of the air and feed solution were found to affect the morphology and dispersion of the samples obtained. The best particle morphology and dispersion were observed when the dry gas inlet temperature, air flow rate, and feed solution flow rate were 55 °C, 660 L/h, and 1.5 mL/min, respectively. The products were broken or even split if the temperature of the dry gas inlet was higher; hollows were formed in the particles at increased air flow rates, and the particle size and dispersion became

worse as the flow rate of the feed solution was increased. The nanocomposites prepared by spray drying under the optimal processing parameters were spheres of 0.2-2 μm in size and composed of 50-100 nm-sized particles. Compared with raw HMX, the optimized sample had a similar crystal structure, a lower melting point, and an insignificantly faster thermal decomposition rate. Meanwhile, the impact sensitivity of the optimized sample was significantly decreased; the critical drop height (H_{50}) had been increased from 18.4 to 56.0 cm.

Acknowledgements
We are grateful for the support of the National Defense Basic Product Innovation Program, Explosive Special Scientific Research Fund.

5 References

[1] Wang J. Y., Huang H., Xu W. Z., Zhang Y. R., Lu B., Xie R.Z., Wang P., Yun N., Prefilming Twin-fluid Nozzle Assisted Precipitation Method for Preparing Nanocrystalline HNS and Its Characterization, *J. Hazard. Mater.*, **2009**, *162*(2-3), 842-847.
[2] Bayat Y., Zeynali V., Preparation and Characterization of Nano-CL-20 Explosive, *J. Energ. Mater.*, **2011**, *29*(4), 281-291.
[3] Li J., Brill T.B., Nanostructured Energetic Composites of CL-20 and Binders Synthesized by Sol Gel Methods, *Propellants Explos. Pyrotech.*, **2006**, *31*(1), 61-69.
[4] Shokrolahi A., Zali A., Mousaviazar A., Keshavarz M.H., Hajhashemi H., Preparation of Nano-K-6 (Nano-Keto RDX) and Determination of Its Characterization and Thermolysis, *J. Energ. Mater*., **2011**, *29*(2), 115-126.
[5] Naya T., Kohga M., Influences of Particle Size and Content of HMX on Burning Characteristics of HMX-based Propellant, *Aerosp. Sci. Technol.*, **2013**, *27*(1), 209-215.
[6] Naya T., Kohga M., Influences of Particle Size and Content of HMX on Burning Characteristics of RDX-based Propellant, *Aerosp. Sci. Technol.*, **2014**, *32*(1), 26-34.
[7] Zohari N., Keshavarz M.H., Seyedsadjadi S.A., The Advantages and Shortcomings of Using Nano-sized Energetic Materials, *Cent. Eur. J. Energ. Mater.*, **2013**, *10*(1), 135-147.
[8] Patrick L., New-generation DuPont Dow Fluoroelastomers: Viton Fluoroelastomer Made with Advanced Polymer Architecture, *Sealing Technology*, **2004**, 5, 6-9.
[9] Craig M.T., Paul A.U., Steven K.C., Leroy G.G., Shock Compression and Initiation of LX-10, *Propellants Explos. Pyrotech.*, **1993**, *18*(3), 117-127.
[10] Sivabalan R., Gore G.M., Nair U.R., Saikia A., Venugopalan S., Gandhe B.R., Study on Ultrasound Assisted Precipitation of CL-20 and Its Effect on Morphology and

Sensitivity, *J. Hazard. Mater.*, **2007**, *139*(2), 199-203.
[11] Degirmenbasi N., Peralta-Inga Z., Olgun U., Gocmez H., Kalyon D.M., Recrystallization of CL-20 and HNFX from Solution for Rigorous Control of the Polymorph Type: Part II, Experimental Studies, *J. Energ. Mater.*, **2006**, *24*(2), 103-139.
[12] Zhigach A.N., Leipunskii I.O., Berezkina N.G., Pshechenkov P.A., Zotova P.A., Kudrov B.V., Gogulya M.F., Brazhnikov M.A., Kuskov M.L., Aluminized Nitramine-based Nanocomposites: Manufacturing Technique and Structure Study, *Combust., Expl. Shock Waves. (Engl. Transl.)*, **2009**, *45*(6), 666-677.
[13] Qiu H.W., Stepanov V., Di Stasio A.R., Chou T.M., Lee W.Y., RDX-based Nanocomposite Microparticles for Significantly Reduced Shock Sensitivity, *J. Hazard. Mater.*, **2011**, *185*(1), 489-493.
[14] An C.W., Li H.Q., Geng X.H., Li J.L., Wang J.Y., Preparation and Properties of 2,6-Diamino-3,5- dinitropyrazine-1-oxide based Nanocomposites, *Propellants Explos. Pyrotech.*, **2013**, *38*(2), 172-175.
[15] Qiu H.W., Stepanov V., Chou T., Surapaneni A., Di Stasio A.R., Lee W.Y., Single-step Production and Formulation of HMX Nanocrystals, *Powder Technol.*, **2012**, *226*, 235-238.
[16] Shi X.F., Wang J.Y., Li X.D., An C.W., Preparation and Characterization of HMX/Estane Nanocomposites, *Cent. Eur. J. Energ. Mater.*, **2014**, *11*(3), 433-442.
[17] Levesque G., Vitello P., Howard W.M., Hot-spot Contributions in Shocked High Explosives from Mesoscale Ignition, *J. Appl. Phys.*, **2013**, *113*(23), 233513.
[18] Li T., Hua C., Li Q., Shock Sensitivity of Pressed RDX-based Plastic Bonded Explosives under Short-duration and High-pressure Impact Tests, *Propellants Explos. Pyrotech.*, **2013**, *38*(6), 770-774.
[19] LaBarbera D.A., Zikry M.A., The Effects of Microstructural Defects on Hot Spot Formation in Cyclotrimethylenetrinitramine-polychlorotrifluoroethylene Energetic Aggregates, *J. Appl. Phys.*, **2013**, *113*(24), 243502.
[20] Yang G.C., Nie F.D., Huang H., Preparation and Characterization of Nano-TATB Explosive, *Propellants Explos. Pyrotech.*, **2006**, *31*(5), 390-394.